Key Engineering Materials
ISSN: 1662-9795, Vol. 1047, pp 161-174

Submitted: 2026-01-18
Accepted: 2026-02-11
Online: 2026-04-13

Development of 3D-Printed Prototype Moulds for Thermoforming

Jan Rösler[1,a*], Jörg Hornig-Klamroth[1,b] and Leon Dähn[1,c]

[1]Berliner Hochschule für Technik, Luxemburger Straße 13, D-13353 Berlin, Germany

[a*]jan.roesler@bht-berlin.de, [b]joerg.hornig@bht-berlin.de, [c]leonskiee@t-online.de

[*]corresponding author

Keywords: thermoforming, prototyping, 3D-printed moulds, PLA, material reduction, cost reduction.

Abstract. The use of 3D-printing simplifies and accelerates the development of moulds for a thermoforming process. This article examines several aspects of the effective design of 3D-printed polymer moulds. The focus is on prototyping and applications in engineering education. Experiments are conducted on PLA mould to determine the actual temperature loads and permanent deformations. Measures to improve the durability of the moulds are discussed and approaches to material and cost optimization are investigated. Examples of the use of PLA-moulds in thermoforming are presented.

Introduction

Thermoforming is an important forming process in plastics processing. It can be used to manufacture small and very large components at low cost. One important area of application is the packaging industry. Components can be manufactured using positive or negative moulds. However, producing the necessary moulds is a complex process. That is why there are activities to produce moulds from plastics using 3D printing, see e.g. [1]. Fused Deposition Modelling (FDM) is widely used in the field of 3D printing. PLA filaments are often used for this process. These filaments are easy to handle, enable detailed printing, and are less likely to warp when cooled. In addition to prototyping, these processes offer the opportunity in academic engineering education to carry out comprehensive, holistic projects covering the entire process chain, from the design of a thermoformed component to mould design and component manufacturing. The flexibility of 3D printing allows students to experimentally optimize mould design and test specific design features. This paper presents the results of several student projects, see Figure 1. In addition, investigations into the durability of PLA moulds are carried out and the influences of several design parameters are analysed in order to design and manufacture mould prototypes more efficiently.

Fig. 1. Example of a thermoformed component produced during a student project (left), massive PLA-mould with 10 mm wall thickness (right), [9].

Vacuum Thermoforming Process

Vacuum thermoforming is a widely used technology to shape plastic films or sheets. During this process the sheet is heated, pre-stretched, and formed, usually assisted with vacuum, cooled and finally demoulded, see [2]. The process is depicted in Figure 2. The demoulding (step 6) can be assisted by applying air pressure.

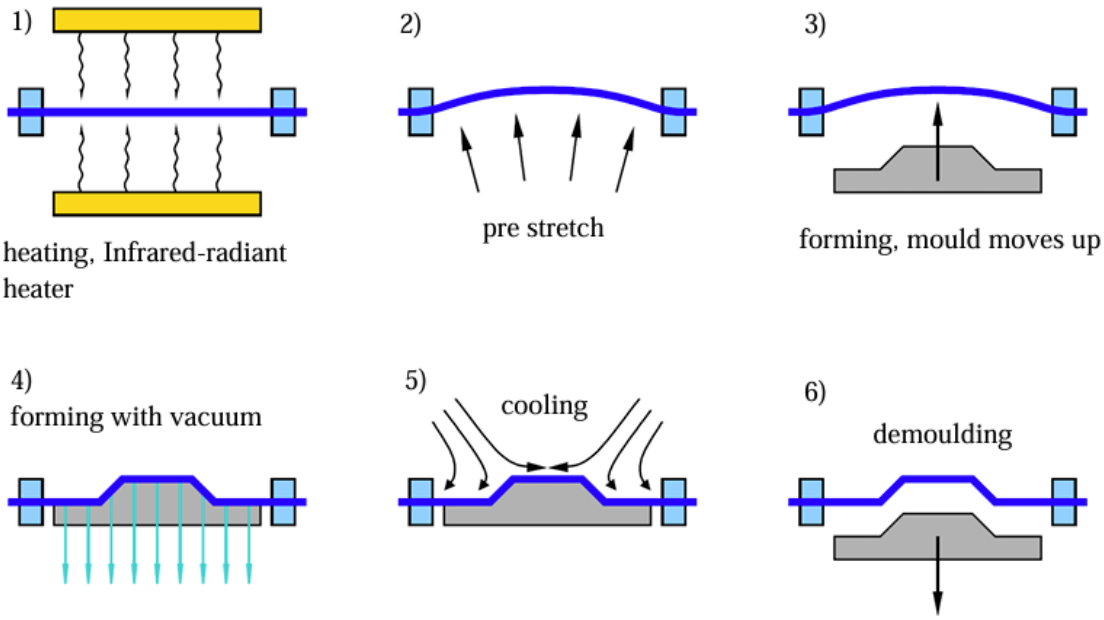

Fig. 2. Vacuum thermoforming process.

For serial production of parts by means of thermoforming, the moulds are manufactured from steel or aluminum by precise 3D machining. This generates high costs, time expenditure and expenses. For prototypes 3D-printed polymer moulds can be an option.

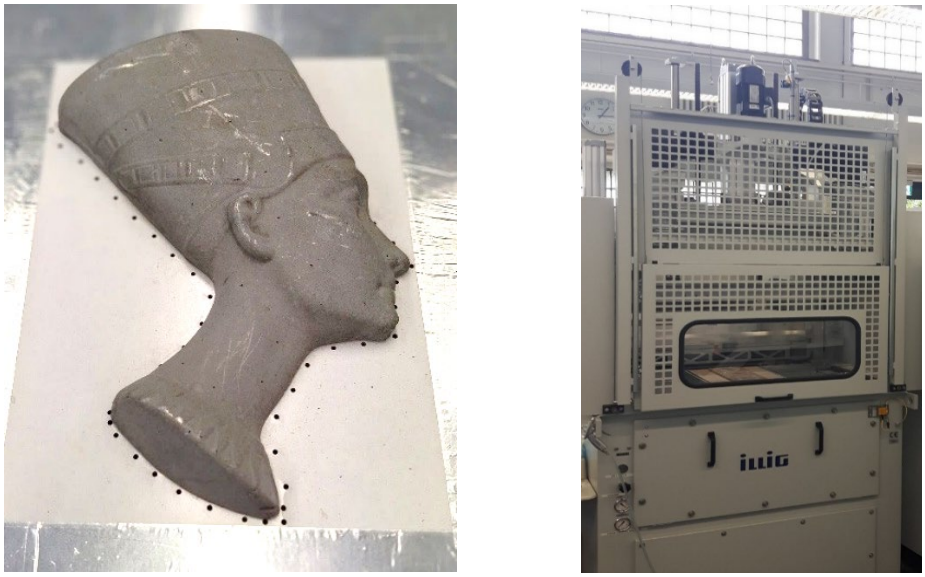

Fig. 3. Conventional aluminum vacuum thermoforming mould (left), Vacuum thermoforming machine Illig UA 100 ed (right).

Investigation of the resistance to thermal and structural loading of 3D-printed PLA vacuum thermoforming moulds

PLA is a popular material for widely used FDM printers. However, it has a relatively low operating temperature. The literature specifies a glass transition temperature (T_g) of approximately 55–60 °C [3] and [4]. The dynamic mechanical analysis (DMA) carried out in our laboratory shows a glass transition temperature T_g of 55°C and a $T_{g\ onset}$ of 51°C. The measurements were carried out using PLA filament pearl-blue from Prusa and the device Netzsch DMA 242 (see Figure 4).

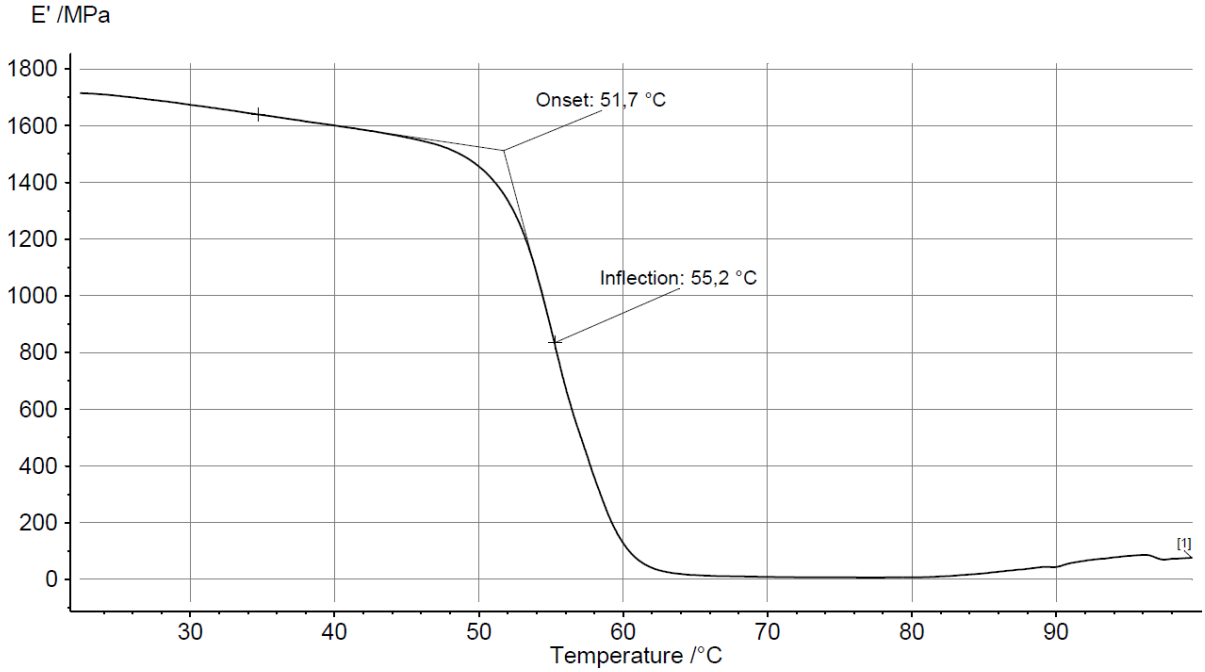

Fig. 4. DMA Analysis of PLA filament - determination of glass transition temperature at a frequency of 1 Hz.

Hence, PLA has a relatively low glass transition temperature and thus temperature resistance compared to other thermoplastics used in the FDM process. For comparison, reference is made to the values for glass transition temperatures given in the literature, e.g.:

- ABS T_g = 105°C … 125°C according [5],
- PET T_g = 70°C … 80°C according [6],
- PETG T_g = 85 according [7]

During the thermoforming process, the sheets are subjected to significantly higher temperatures. The Illig UA 100Ed used here, see Figure 3 (right), has IR emitters with a heating capacity of 400–525°C (bottom and top heating). The processing temperatures for the sheets are significantly lower, but with a temperature range of 110°C to 190°C for PETG sheets (see [2]) they are considerably above the glass transition temperature of PLA T_g = 55°C.

The question arises as to what temperatures can occur in the mould during the thermoforming process? What design should a PLA mould have to function properly? What configurations, thickness, infill density and pattern, as well as structural design, are necessary for optimal results with low material costs and printing time? In the tests described below, PLA moulds are subjected to a challenging test program in order to help clarify these questions.

Design of analysed PLA thermoforming moulds

Four different types of PLA-Thermoform moulds were investigated. The basic geometry is depicted in Figure 5.

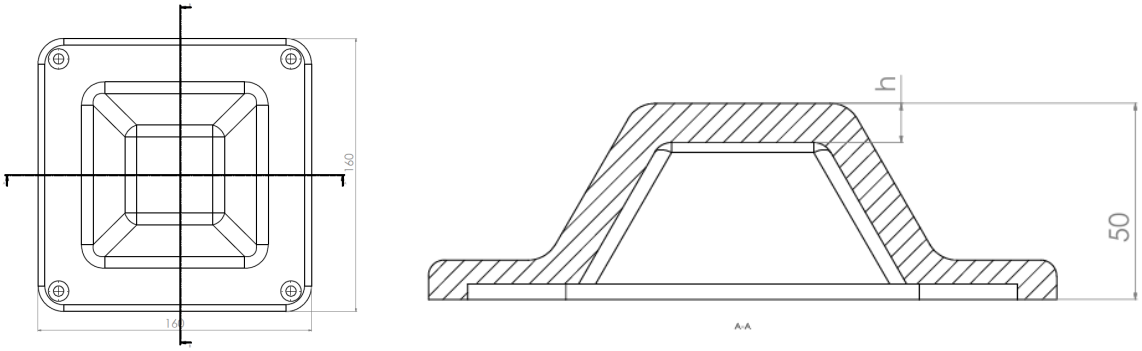

Fig. 5. General geometry of considered PLA-moulds.

The distinguishing feature of the moulds are

1. wall thickness h = 1.5 mm printed with 100% infill
2. wall thickness h = 3.0 mm printed with 100% infill
3. wall thickness h = 10 mm printed with 15% infill
4. wall thickness h = 5 mm printed with 100% infill

While the moulds 1, 2 and 4 are monolithic, printed with 100% infill, the mould No. 4 has an internal honeycomb structure with 15% infill, see Figure 6. The moulds were attached to the wooden base plate of the thermoform machine by means of screws and sealed with aluminum tape (see Figure 8 c).

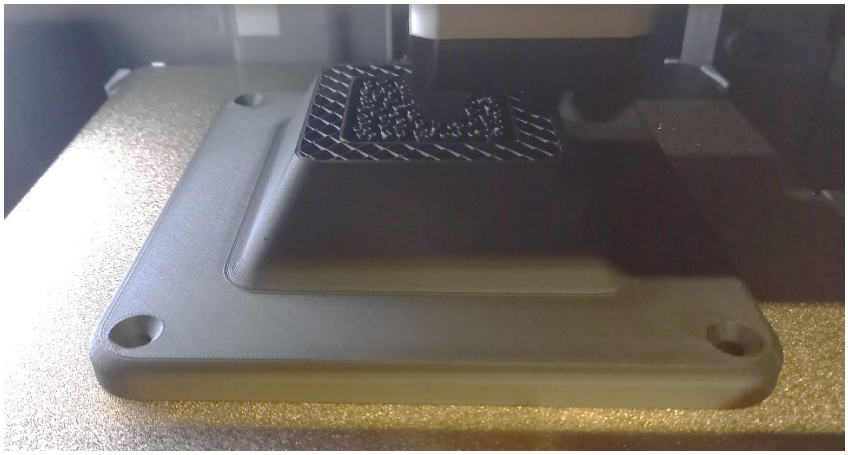

Fig. 6. Printing mould No. 3 with 15% infill and honeycomb pattern.

Since for prototyping the time expenditure is of great importance, the estimated printing times of all four moulds were compared. This is based on the output of the Bambu Lab Studio software. The CAD-models of the four moulds were sliced, yielding an estimation of time and filament mass estimated by the slicing software. Additionally, the required masses of PLA-filaments were analysed. Both, relative printing time and filament mass are depicted in Figure 7. The data are related to a mould design with 10 mm wall thickness and 100% infill, referenced as model 5. Compared to this robust and heavy design, the proposed designs of mould 1 to mould 4 result in considerable reductions. However, these savings come with effects on durability, to be discussed next.

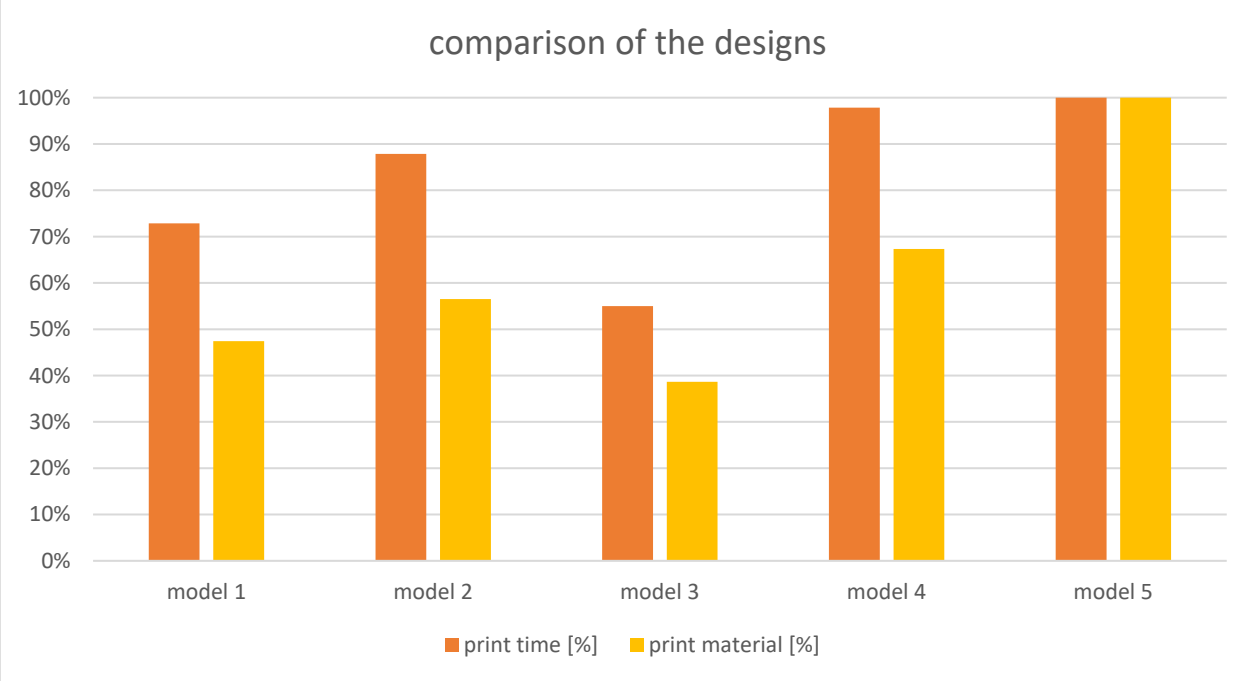

Fig. 7. Comparison of designs – printing time and mass of used filament.

Experimental design and measurement methods

If PLA is to be used for thermoforming moulds, it is useful to determine the temperatures that can be expected during thermoforming in a polymere mould. For this reason, temperature measurements were taken on PLA-moulds during the thermoforming process inside the mould. During the series of measurements, temperatures in the inner of a mould T_1 and T_2 were recorded at two positions inside the mould (see Figure 8 a). The temperatures were measured using a Voltcraft K 202 thermometer with data logger and K-type thermocouples. The measuring device was placed inside the mould base plate of the thermoforming machine to continuously record the temperature.

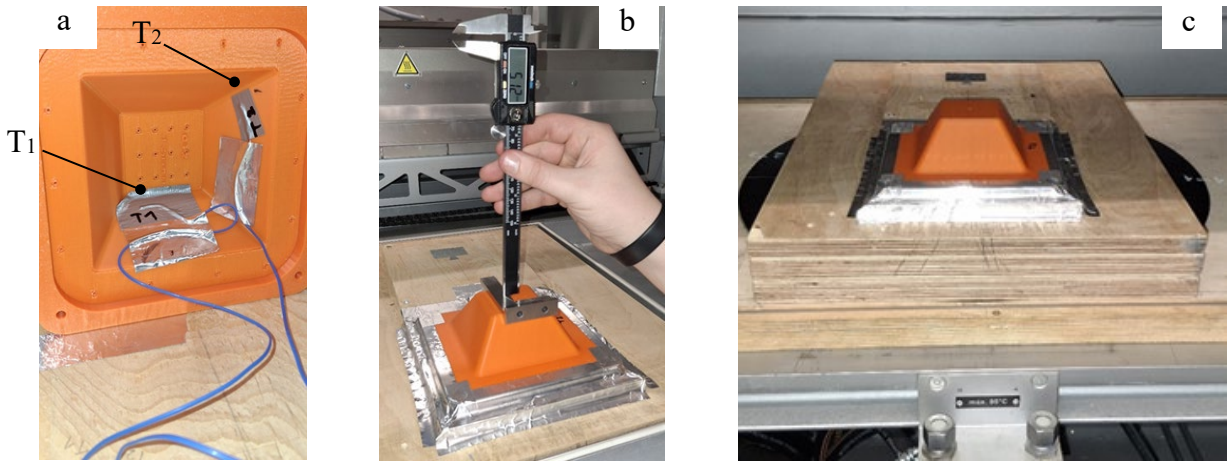

Fig. 8. (a) Position of thermoelements T_1 and T_2, (b) measurement of deflection of the top plate with digital calliper, (c) mould installed in the thermoforming machine Illig UA 1100 ed.

In addition, the temperatures on the surface of the thermoformed sheet and on the top of the mould were measured using a Flir E4 infrared camera. This measurement was taken after completion of the thermoforming process, i.e. after cooling and demoulding of the sheet. In order to analyse the durability of the PLA mould, the deformations of the top plate of the mould were measured with a calliper depth gauge after each thermoforming cycle. The moulds were subjected to a 3-minute cycle. This includes the entire thermoforming process and a subsequent cooling phase, during which the measurements were taken and the next cycle was prepared.

Thermoforming process and test program

The thermoforming processed with a vacuum thermoforming machine Illig UA 100 Ed using the parameters given in Table 1.

Table 1. Process parameters for thermoforming process.

Material	PETG sheet 540 mm × 400 mm, thickness 0.75–0.8 mm (see Figure 20)	
Heater settings	upper heater: 3 zones at 360 °C	lower heater: 3 zones at 360 °C
Heating time	22 s per cycle	
Pre-blow	activation after 0 s	duration approx. 0.5 s
Vacuum delay and duration	vacuum applied with ca. 4 s delay (active during forming phase)	
Cooling time	8 s	
Demoulding air	1 s	

In total this thermoforming process lasts approx. 45 s. In the course of the test series 3-minutes cycles were run. Here, the detailed description of the test program for every of the four moulds will be given:

Mould No 1

This mould was exposed to two cycles until its failure. The internal temperatures T_1 and T_2 were measured.

Mould No. 2

It was exposed to 6 cycles. An additional cycle was interrupted due to failure. The internal temperatures T_1 and T_2 were recorded.

Mould No. 3

Ten cycles were carried out with this mould.

Mould No. 4

This mould was run 10 cycles of 3 minutes, except one 5 minutes interval between cycles 8 and 9. The internal temperature T_1 was measured.
The temperature at the top and the temperature of the processed PETG-sheet was measured direct after thermoforming for all four moulds. Furthermore, the permanent deflection in the centre of the top plate was determined.

Experimental analysis of thermal behaviour of PLA-moulds

Mould No. 1

With a wall thickness of 1.5 mm failed in the second cycle. After the first cycle, a temperature of T = 58 °C was measured on the mould surface, which rose to 62 °C in the second cycle. The mould deformed significantly, meaning that the test series could not be continued.

Mould No. 2

Temperatures inside the mould during thermoforming were examined for mould No. 2 with a wall thickness of 3 mm and 100% infill. The temperature curves T_1 und T_2 can be seen in Figure 9. Over the course of six cycles, a maximum temperature of 61°C was measured inside the mould. This is significantly above the glass transition temperature.

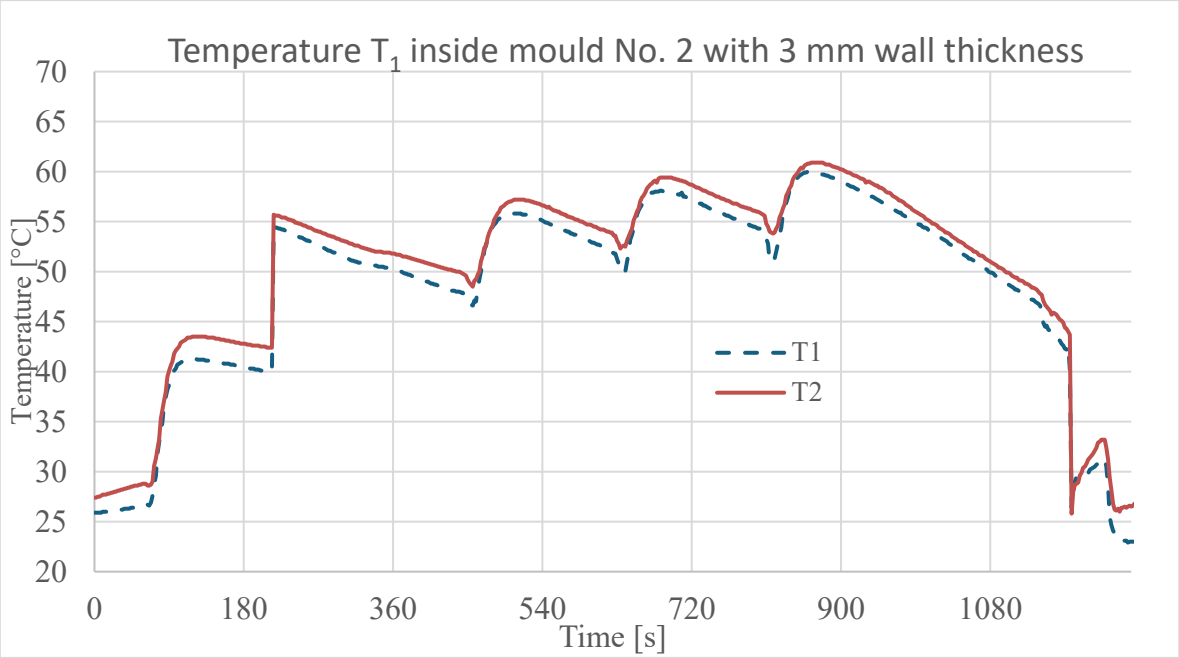

Fig. 9. Temperature in the inner of mould No. 2 (h=3mm).

The temperatures on the top of the mould and on the upper surface of the sheet were measured immediately after a thermoforming process by means of IR-camera (see Figure 10).

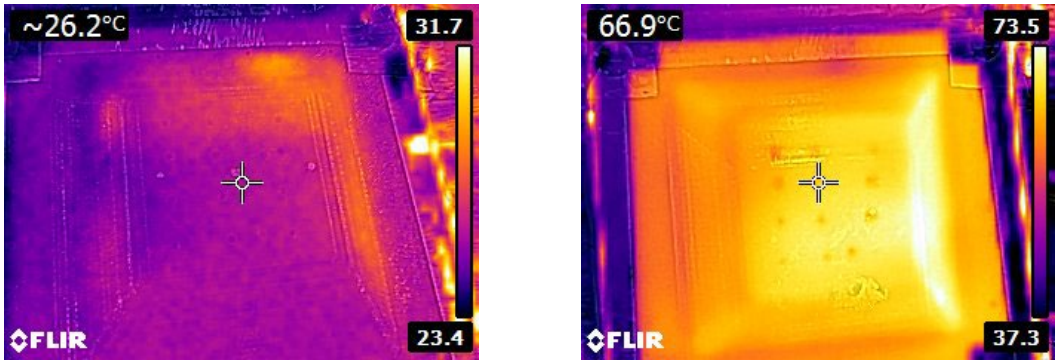

Fig. 10. IR-Photograph of mould No. 2 bevor the 1st. and after the 6th cycle (top view).

An overview of these temperatures for all cycles is given in Figure 11. The top of the mould heats up to almost 70°C.

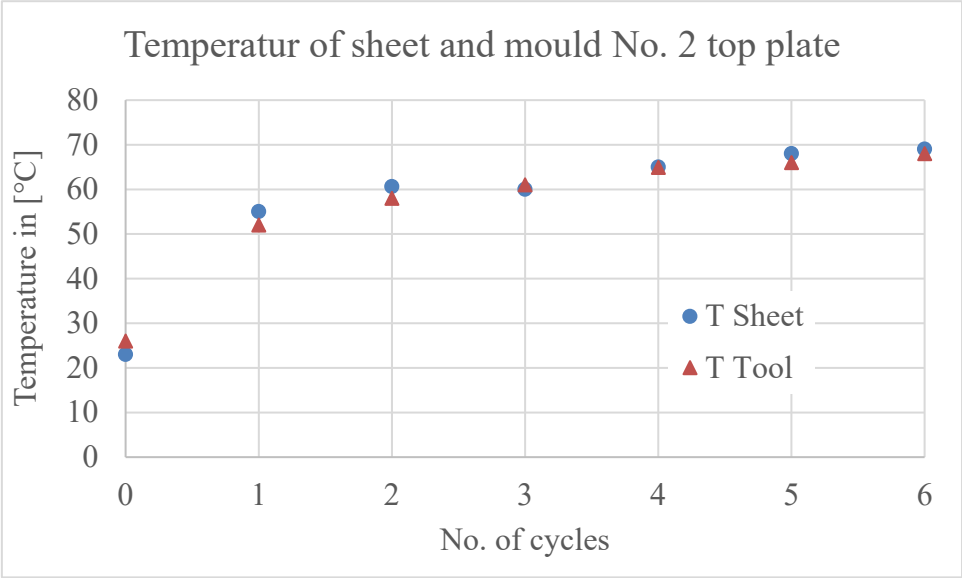

Fig. 11. Temperature of mould No 2 (h = 3mm) top plate and the thermoformed sheet after finishing a cycle.

This significantly exceeds the glass transition temperature. After six cycles, the test series was discontinued due to excessive deformation of the mould. The associated structural mechanical behaviour is discussed below.

Mould No. 3

Here too, the temperatures on the surface of the films and the mould were measured after each thermoforming cycle. Figure 12 shows the temperatures on the sheet and mould surface for 10 cycles. The temperatures on the mould surface reach up to 77°C, which is 10°C above the maximum temperature of mould No. 2. After three cycles, the surface temperature is 70°C, compared to 61°C after three cycles with mould No. 2. (see Figure 11). The cause of this is believed to be the internal structure of the mould, forming closed honeycomb cells. This structure reduces the thermal conductivity of this sandwich-like structure compared to the conductivity of the monolithic structure of mould No. 2.

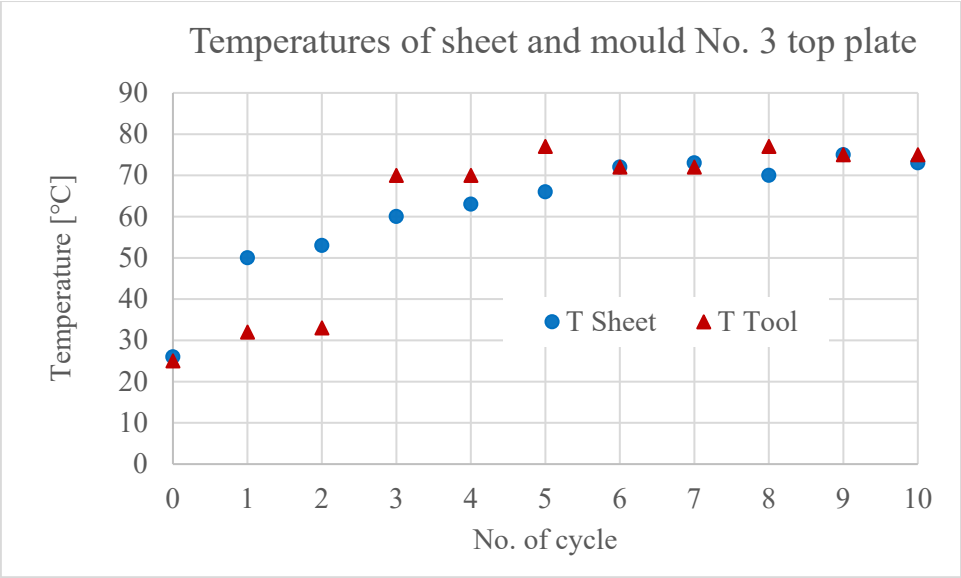

Fig. 12. Temperature of mould No. 3 Top plate and thermoformed sheet after finishing a cycle.

Mould No. 4

The temperature T_1 on the inside of the mould (Figure 13) reaches a maximum of 58°C after 8 cycles and is therefore still lower than the maximum external surface temperature on the mould. Temperature T_1 was not recorded for the remaining last two cycles.

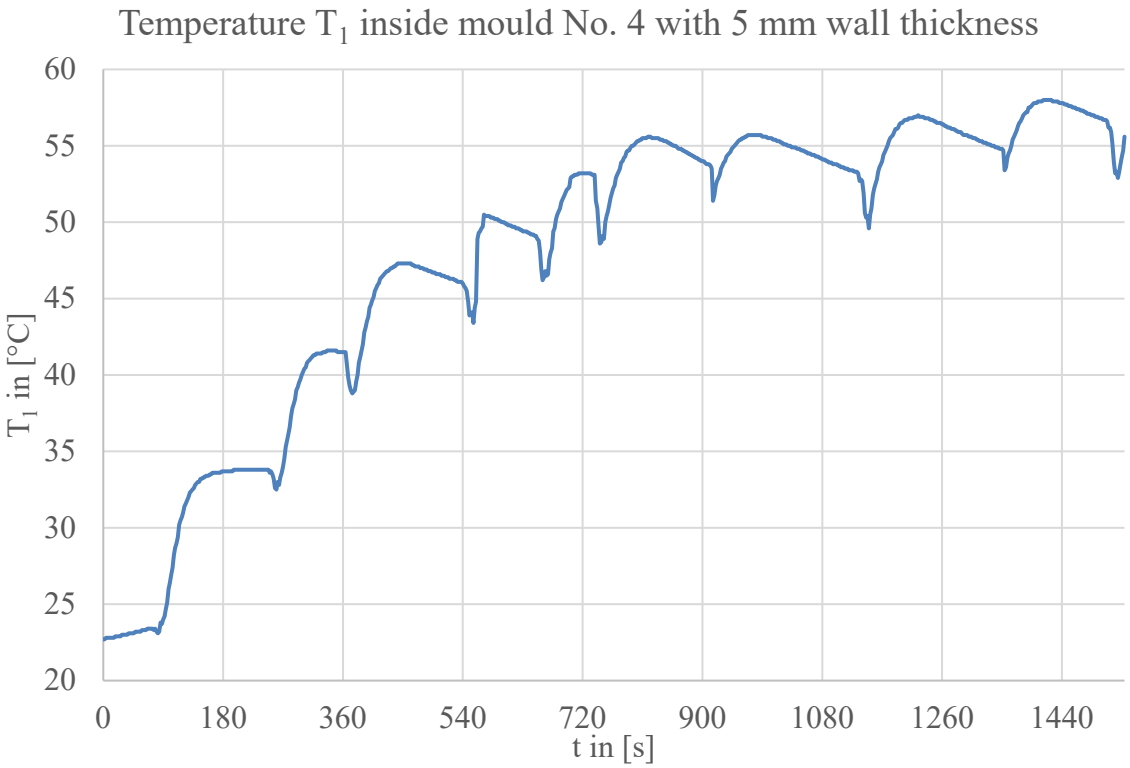

Fig. 13. Temperature in the inner of mould No. 4 (h=5mm).

Figure 14 shows the temperatures at the sheets and mould surface. The temperatures at the mould surface reach up to 66°C, which is slightly higher than for mould No. 2. After three cycles, the surface temperature is 57°C, compared to 61°C after three cycles for mould No. 2.

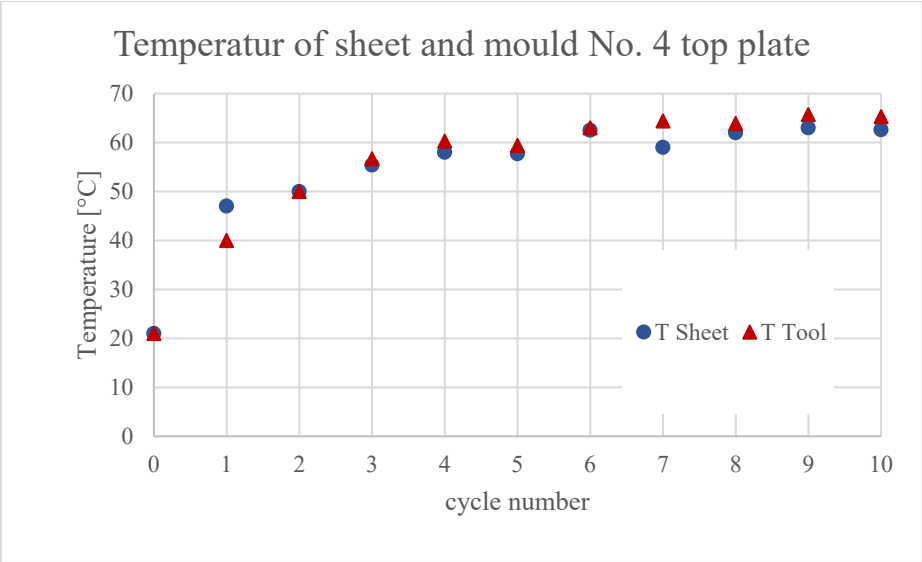

Fig. 14. Temperature of mould No. 4 (h=5mm) Top plate and thermoformed sheet after finishing a cycle.

Structural behaviour of PLA-Moulds and thermoformed PETG-sheets

Mould No. 1

In the tests the mould collapsed during the second cycle (see Figure 15 left). Significant deformation of the side walls and top plate is visible. The mould became unusable.

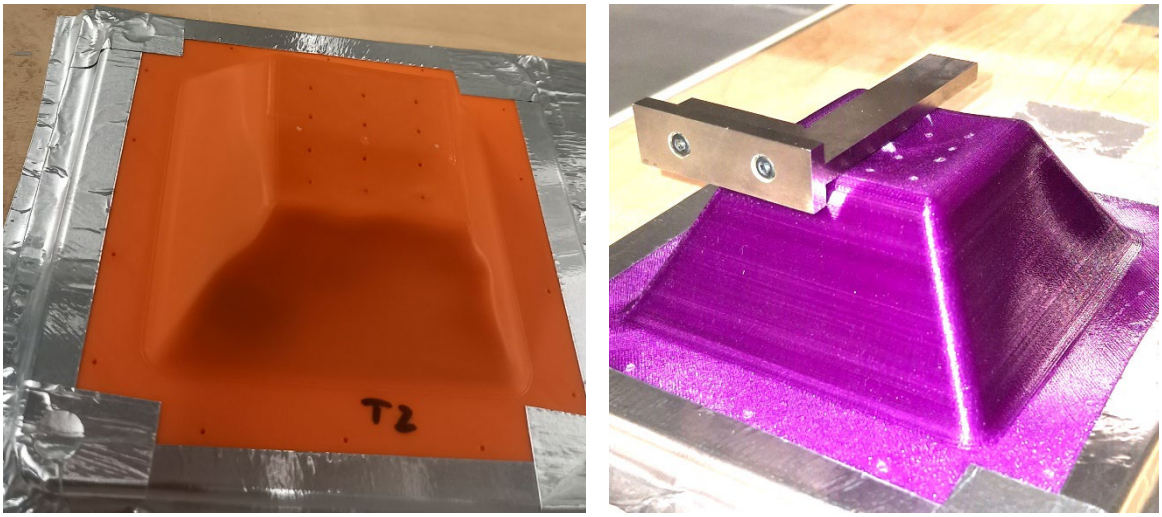

Fig. 15. Mould No. 1 after collapse during the 2nd cycle (left), mould No. 2 after 6 cycles showing deformation of the top plate and of the sidewalls (right).

Mould No. 2

During the six test cycles of mould No. 2, an increasing plastic deflection of the top plate was observed. The development of this deflection is shown in Figure 16. The deformed state of the moulds top plate after 6 cycles is depicted in Figure 15 (right). Beside deflections of the top plate a deformation of sidewalls is visible. This deformation caused some problems during demoulding of the sheet occurring during cycle 4 and the following cycles.

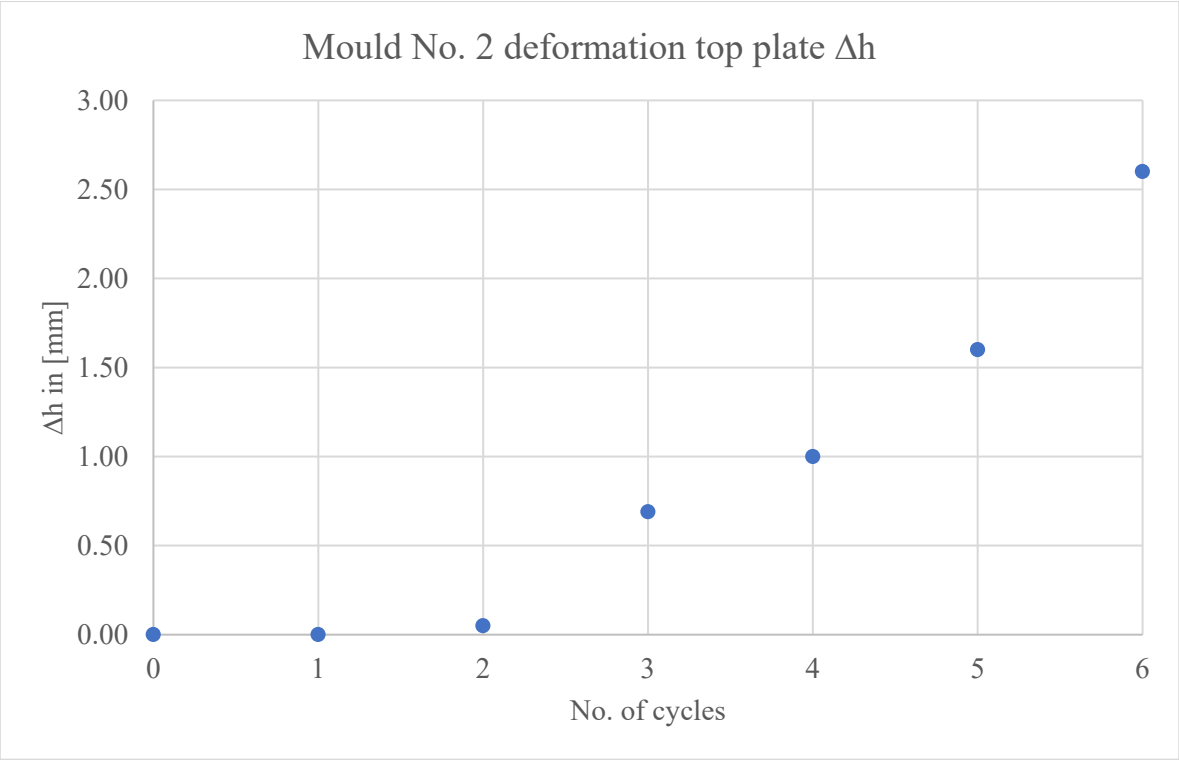

Fig. 16. Deflection of top plate of mould No. 2 (h = 3 mm).

Mould No. 3

In tests with structural design, the structure proved to be only partially effective. Indentations appeared between the cell-like structural elements, depicted in Figure 17. As a result, the moulded components became stuck partially after six cycles. However, the basic shape of the mould remained intact. Because of the local deformation the permanent deflection of the top plate Δh was not analysed for this mould.

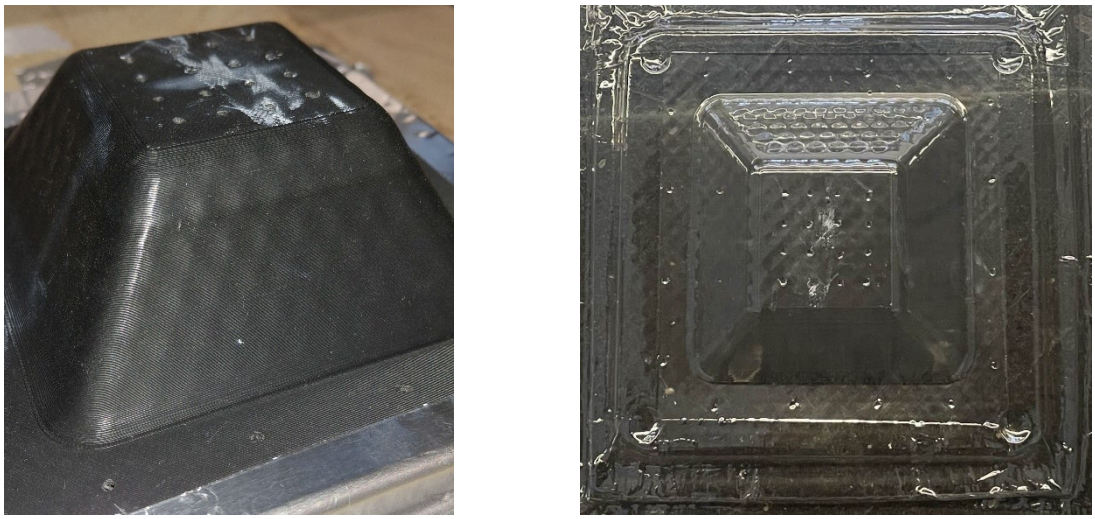

Fig. 17. Mould No. 3 after 2 cycles outer skin with honeycomb pattern at surface (left), thermoformed sheet showing imprint of honeycomb pattern (right).

Mould No. 4

Tests with this design showed significantly higher resilience during thermoforming. Eight cycles could be carried out without any problems. After that, deformations appeared in the base, leading to difficulties in demoulding. This can be eliminated by simple reinforcements.

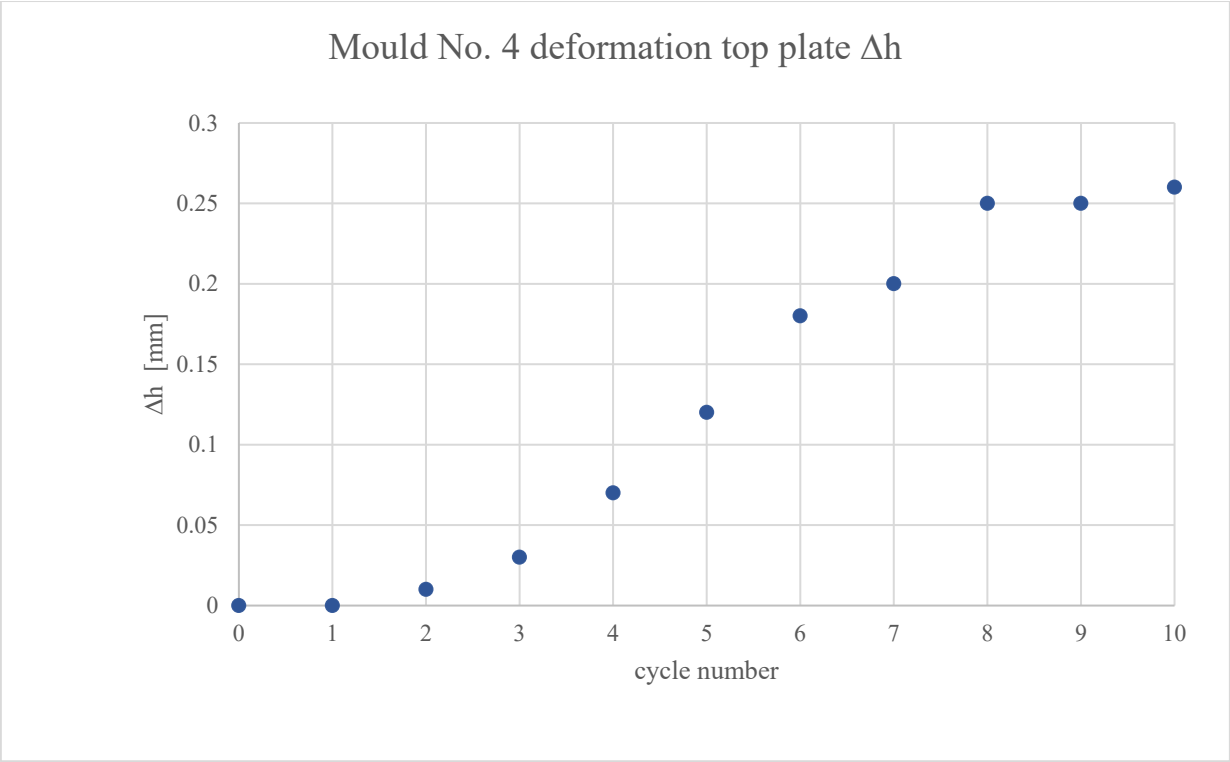

Fig. 18. Deflection of top plate of mould No. 4 (h=5 mm).

Figure 18 shows the deflection of the top plate of the mould. Compared with other designs, the deformations are small. However, the critical deformation occurred at the base of the mould, as shown in Figure 19.

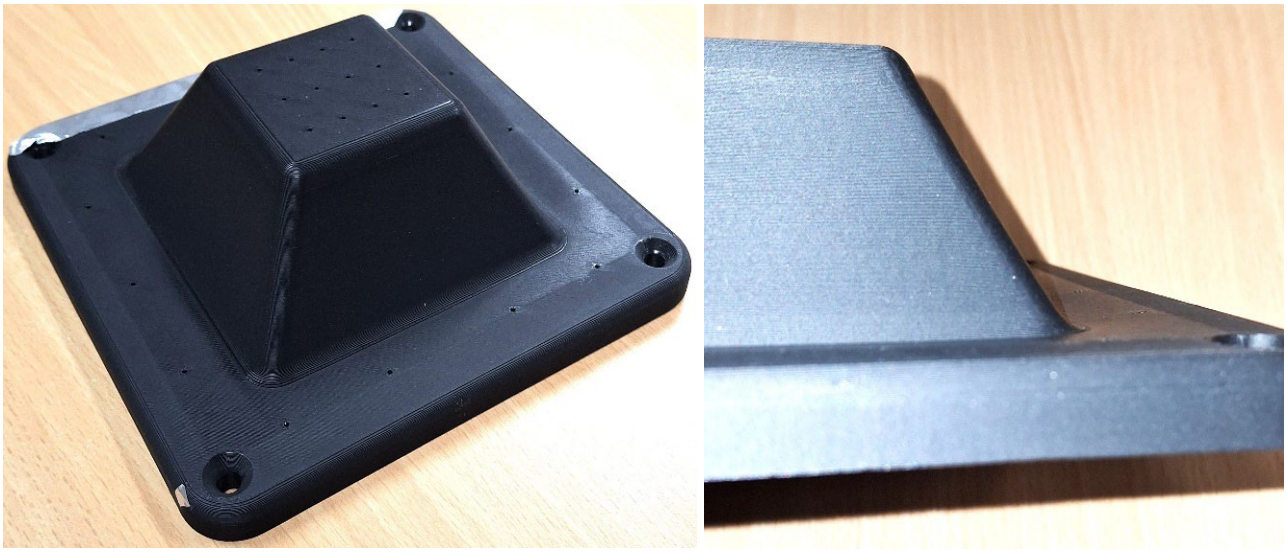

Fig. 19. Mould No. 4 after tests, deformation at the mould base.

Deformation of the thermoformed PETG-sheets:

To analyse the deformations, a grid with a 20 mm × 20 mm grid was drawn on a sheet. After thermoforming, this grid is distorted. Figure 20 shows the undeformed (left) and deformed grid (middle).

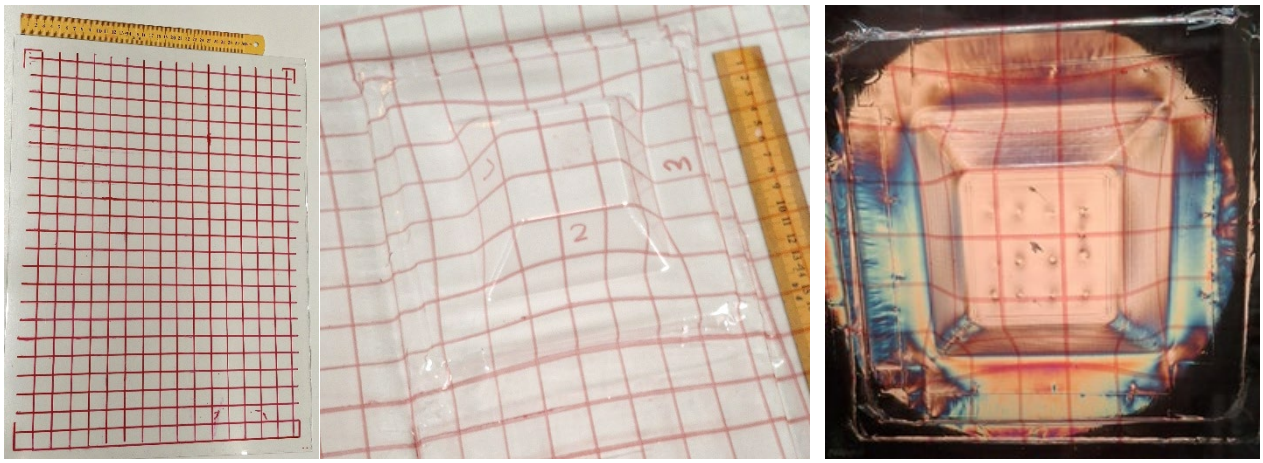

Fig. 20. Undeformed sheet 540 mm × 400 mm with mesh (left), State of deformation of the thermoformed sheet (middle) and orientations in polarized light (right).

For fields 1, 2 and 3 marked in Figure 20 (middle), the changes in length and thickness were measured and the resulting degrees of deformation were determined according [8].

$$\varphi = \ln\left(\frac{x_1}{x_0}\right) = \ln\left(1 + \frac{\Delta x}{x_0}\right) \quad (1)$$

Here x_0 and x_1 are length in undeformed and deformed state respectively.

Table 2. Change of dimensions and degree of deformation for fields 1, 2 und 3.

	field No. 1	field No. 2	field No. 3
$\Delta\ell$ [mm]	7	0	6
φ_x [1]	0,3	0	0,26
Δb [mm]	0	6	0
φ_y [1]	0	0,26	0
Δt [mm]	0.11	0.08	0.09
φ_z [1]	-0.15	-0.11	-0.12

Results are given in Table 2. This analysis clearly shows significant local stretches of the sheets, thereby reducing the wall thickness. These deformations are accompanied by changes in the internal structure. The orientations can be made visible in a polariscope. Figure 20 (right) shows significant stretching of the material in the base area. Despite the symmetrical shape, the orientation is asymmetrical because the mould is not centred on the base plate of the thermoforming machine, i.e. there are different distances between the clamping points for the sheets in the clamping frame. At the same time, the heating effect of the IR radiators may vary in the centre and at the edge of the temperature field.

Applications – development of thermoformed products in academic engineering education

Example A: One project involved developing thermoformed packaging and the corresponding thermoforming mould. Figure 21 [9] shows an example of this product development. The task required the design of clip connections for closing the packaging. Various geometries and dimensions of the clip connection were tested. 3D printing enabled the flexible production of thermoforming moulds for experimental parameter studies. This made it possible to easily produce various parts using thermoforming and determine the optimal geometry for the desired assembly and disassembly forces. There was no need for complex metal moulds or simulations.

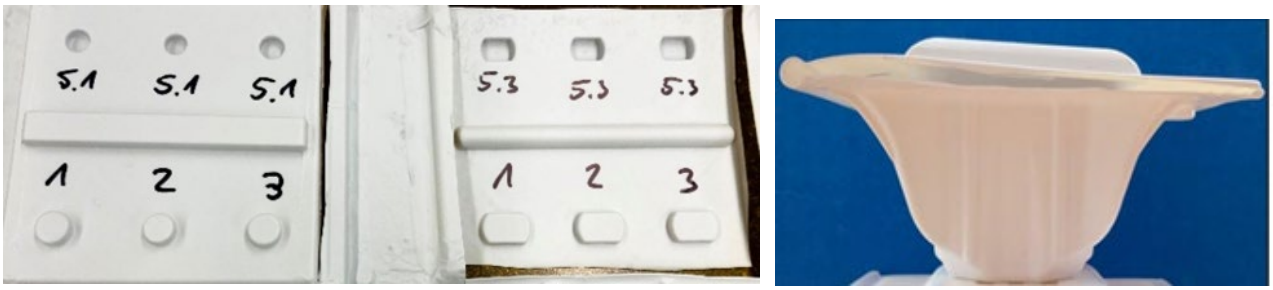

Fig. 21. Series for different geometries of clip connections (left), Example of packaging manufactured using thermoforming and 3D printed moulds (right).

Example B: The aim of this project was to design buckets for wall paint that are easy to clean. This facilitates subsequent recycling and increases the quality of the recycled material. For this study, moulds were produced using 3D printing and used to manufacture scaled bucket parts by thermoforming (see Figure 22 [10]). These samples were used to test the suitability of the different designs for cleaning.

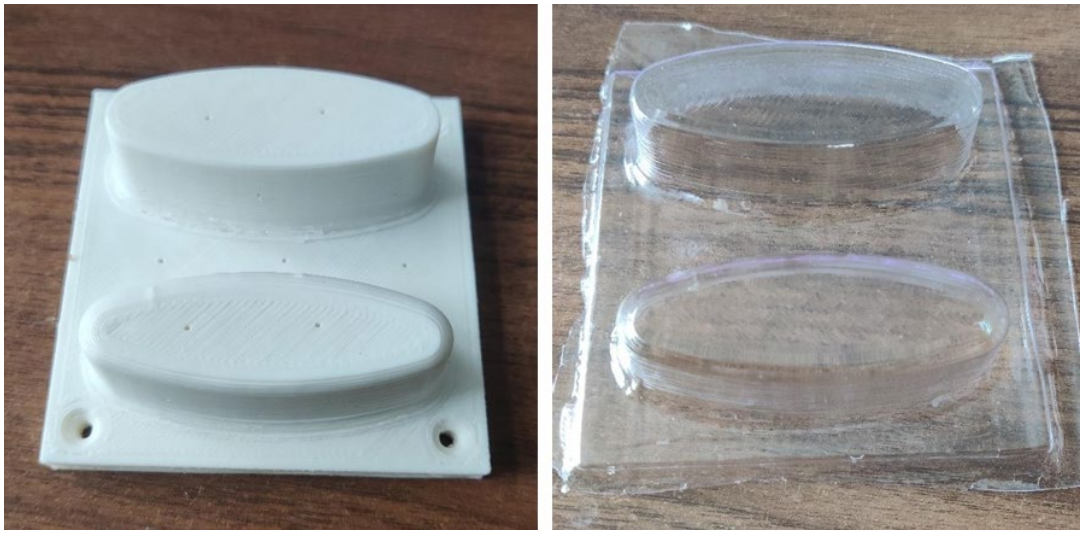

Fig. 22. Printed mould (left) and thermoformed parts (right).

Summary

PLA moulds were successfully used in both projects. The flexibility of 3D printing enables detailed experimental investigations of the different designs. In the practical implementation of these projects, the cycle times were significantly less critical than in the tests carried out. The experiments showed that when using PLA moulds in thermoforming, the structure and process temperatures have a significant influence on their service life. The results obtained contribute to the efficient design of 3D-printed prototype moulds for thermoforming. The following guidelines for polymer mould design can be derived from this.

- the outer skin of the mould should be solid or with dense infill to avoid local deformations and distortion of the outer mould shape.
- to keep dimensional stability and improve structural integrity stiffeners as ribs or supporting structure inside the mould are highly recommended.
- the inner structure of the mould should enable heat transfer, closed cells shall be avoided.
- materials with high glass transition temperature are advisable.

A very simple method of reducing the temperature loads of the mould was to cool it briefly with a damp cloth. This led to a rapid drop in temperature.

References

[1] N.N.: Schnelles Thermoformen in Kleinserie mit 3D-gedruckten Formwerkzeugen, formlab, [online], https://formlabs.com/de/white-papers/low-volume-rapid-thermoforming-with-3d-printed-molds/, 17th January 2026.

[2] Illig, A. (ed.): Thermoformen in der Praxis, München, Wien, Hanser 1997.

[3] Demiryurek, S.G: Evaluation of dynamic properties in ABS and PLA thermoplastics across frequency ranges. Sci Rep 15, 42629, 2025, https://doi.org/10.1038/s41598-025-26846-9.

[4] Khouri N. G, Bahú J. O, Blanco-Llamero C, Severino P, Concha V. O. C: Polylactic acid (PLA): Properties, synthesis, and biomedical applications – A review of the literature, Journal of Molecular Structure Vol. 1309, 2024, https://doi.org/10.1016/j.molstruc.2024.138243.

[5] Erhard, Gunter: Konstruieren mit Kunststoffen, 4. Auflage, Carl Hanser Verlag, 2008.

[6] Ehrenstein, G W.: Mit Kunststoffen konstruieren, 3. Auflage, Carl Hanser Verlag, 2007.

[7] N.N. PETG filament data sheet, BigRep GmbH, [online], www.bigrep.com/filaments/petg, 17th January 2026.

[8] Bender B, Göhlich D (eds.): Dubbel Taschenbuch für den Maschinenbau 2: Anwendungen Springer Vieweg Berlin, Heidelberg 2020, https://doi.org/10.1007/978-3-662-59713-2.

[9] Kollmeier S, Wolf J, Schnellbach Dennis, Bernstein J: Konstruktive Aufgabe: Transportverpackung, Wintersemester 2024/25, Berliner Hochschule für Technik, 2025.

[10] Hannes B. K, Heinrich J. P: Recyclinggerechte Werkstoffgestaltung eines Farbeimers, Sommersemester 2025, Berliner Hochschule für Technik, 2025.

The publication of this article was funded by the Berlin University of Applied Sciences